Fragmentation of multiply-charged small hydrocarbon molecules C_nH^{q+} (n=1-3, q=2-6) produced in high velocity collisions: Branching ratios and kinetic energy releases of the H^+ fragment

K.Béroff[1], M.Chabot[2], T.Pino[1], N.G.Van-Oanh[3], T.Tuna[2], A.Le Padellec[4], P.Désesquelles[5],G.Martinet[2]

[1]Institut des Sciences Moléculaires, CNRS and University Paris Sud, 91405 Orsay (France)
[2]Institut de Physique Nucléaire, CNRS-IN2P3 and University Paris Sud 91406 Orsay Cedex (France)
[3]Laboratoire de Chimie Physique CNRS and University Paris Sud, 91405 Orsay (France)
[4]Centre d'Etudes spatiales des rayonnements CNRS and University Toulouse III, F-31028 Toulouse Cedex (France)
[5]Centre de Spectrométrie Nucléaire et de Spectrométrie de masse, CNRS-IN2P3 and University Paris Sud, 91405 Orsay Cedex (France)

In a recent work (Chabot et al this conference and PRL **104**, 043401 (2010)), we showed how fragmentation of multi-charged carbon clusters C_n^{q+} strongly evolves with the strength of the coulomb interaction. In this work, we pursued these studies on new C_nH^{q+} species (n=1-3, q=2-6) and added a new experimental observable: the kinetic energy release of the H^+ fragment KER-H^+, extracted for each dissociation channel.

Experimental method

AGAT set-up at the Tandem accelerator in Orsay

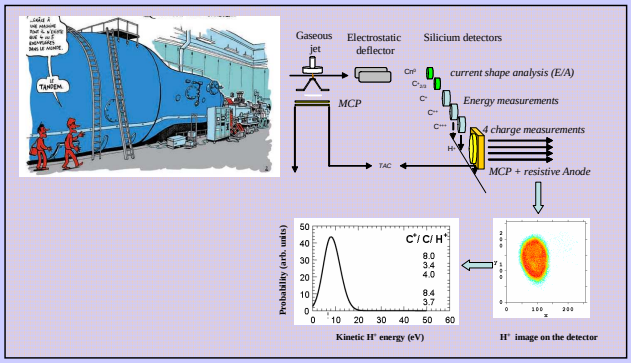

Ionization cross sections

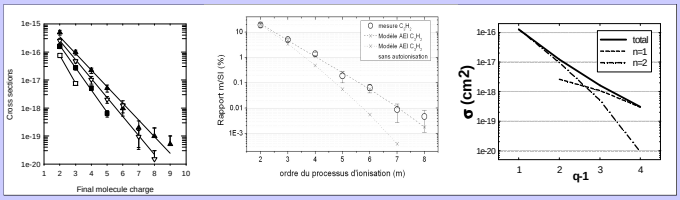

Measured ionization cross sections of in C_nH^{q+} -He collisions at v=4.5 a.u; lines are to guide the eye (left). Comparison between measured and calculated (IAE model) ionization cross sections in $C_3H_2^+$ at v=4.5a.u (middle). Calculated (IAE model) valence and 1s ionization cross sections in CH^+-He at v=3.6 a.u (right)

KER-H^+ measurements

& comparison with the point charge coulomb model

Mol.	Charge	Channel	E1c (eV)	σ1 (eV)
CH	1	C/H^+	4.0	3.0
	2	C^+/H^+	7.9	2.7
	3	C^{++}/H^+	16.4	6.5
	4	C^{+3}/H^+	20.7	8.4
C_2H	1	C_2/H^+	0.9	2.8
		$C/C/H^+$	1.2	3.1
	2	C_2^+/H^+	6.0	2.0
		$C^+/C/H^+$	8.4	3.7
	3	$C^+/C^+/H^+$	15.1	4.7
		$C^{++}/C/H^+$	15.1	6.6
	4	$C^{++}/C^+/H^+$	21.4	7.6
		$C^{+3}/C/H^+$	11.4	13.3
	5	$C^{++}/C^{++}/H^+$	27.8	9.3
		$C^{+3}/C^+/H^+$	24.5	10.2
	6	$C^{+3}/C^{++}/H^+$	31.8	10.9
	7	$C^{+4}/C^{+3}/H^+$	37.7	7.1
C_3H	1	C_3/H^+	1.5	1.4
		$C_2/C/H^+$	1.3	2.1
		$C/C/C/H^+$	6.5	6.6
	2	C_3^+/H^+	8.5	4.2
		$C_2^+/C/H^+$	6.1	2.7
		$C^+/C_2/H^+$	5.3	2.5
		$C^+/C/C/H^+$	7.3	3.3
	3	$C_2^+/C^+/H^+$	10.7	3.5
		$C^+/C^+/C/H^+$	12.7	3.8
		$C_2/C^{++}/H^+$	9.7	6.2
		$C^{++}/C/C/H^+$	12.9	4.2
	4	$C^+/C^+/C^+/H^+$	18.4	6.6
		$C_2^+/C^{++}/H^+$	13.1	8.1
		$C/C^+/C^{++}/H^+$	17.3	8.5
	5	$C^+/C^+/C^{++}/H^+$	23.4	9.1
		$C/C^{++}/C^{++}/H^+$	28.0	4.4
	6	$C^+/C^{++}/C^{++}/H^+$	29.4	9.5
		$C^+/C^+/C^{+++}/H^+$	26.1	11

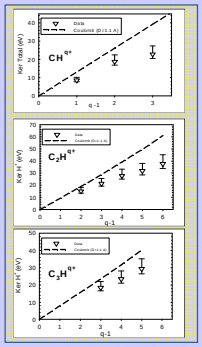

Characteristics of measured KER-H^+ distributions for various dissociation channels of C_nH^{q+} molecules. A Gaussian shape (E1c: peak position, σ1: standard deviation was assumed) (left)

Comparison between measured KER values and predictions of the point charge coulomb model (PCCM) (right)

KER calculations (CH^{q+} case)

State	CH^+	CH^{++}	CH^{3+}	CH^{4+}
Ground state	$X^1\Sigma^+$ (0) $(1\sigma^2\,2\sigma^2\,3\sigma^2)$	$1\,^2\Sigma^+$ (0)*, ** $(1\sigma^2\,2\sigma^2\,3\sigma)$	$1\,^1\Sigma^+$ (0)*,** $(1\sigma^2\,2\sigma^2)$	$1\,^2\Sigma^+$ (0)*,** $(1\sigma^2\,2\sigma)$
First Excited state	$a^3\Pi$ (0.98) $(1\sigma^2\,2\sigma^2\,3\sigma\,1\pi)$	$1^2\Pi$ (3.6)** $(1\sigma^2\,2\sigma^2\,1\pi)$	$1\,^3\Sigma^+$ (5.9)*,** $(1\sigma^2\,2\sigma\,3\sigma)$	$2\,^2\Sigma^+$ (11)*,** $(1\sigma^2\,3\sigma)$
Second excited state		$2\,^2\Sigma^+$ (10)* $(1\sigma^2\,2\sigma\,3\sigma^2)$	$1\,^3\Pi$ (8.4)** $(1\sigma^2\,2\sigma\,1\pi)$	$1\,^2\Pi$ (12.1)** $(1\sigma^2\,1\pi)$
Third excited state		$2\,^2\Pi$ (13.1)** $(1\sigma^2\,2\sigma\,3\sigma1\pi)$	$2\,^1\Sigma^+$ (10.1)*, ** $(1\sigma^2\,2\sigma\,3\sigma)$	$3\,^2\Sigma^+$ (31.7) $(1\sigma^2\,4\sigma)$
Fourth excited state		$3\,^2\Pi$ (15.2)** $(1\sigma^2\,2\sigma\,3\sigma\,1\pi)$	$1\,^1\Pi$ (13.5)** $(1\sigma^2\,2\sigma\,1\pi)$	
Fifth excited state		$1\,^2\Delta$ (16) $(1\sigma^2\,2\sigma\,1\pi^2)$	$2\,^3\Pi$ (20.5)** $(1\sigma^2\,3\sigma\,1\pi)$	
Sixth excited state		$3\,^2\Sigma^+$ (17.5) $(1\sigma^2\,2\sigma^2\,4\sigma)$	$3\,^1\Sigma^+$ (21.1)* $(1\sigma^2\,3\sigma^2)$	
Seventh excited state		$1\,^2\Sigma^-$ (18.2) $(1\sigma^2\,2\sigma\,1\pi^2)$	$1\,^3\Sigma^-$ (22.85) $(1\sigma^2\,1\pi^2)$	
Eigth excited state			$2\,^1\Pi$ (24.3)** $(1\sigma^2\,3\sigma\,1\pi)$	

Calculated electronic excited states of CH^+, CH^{++}, CH^{+++} and CH^{4+} by the CASSCF method using the MOLPRO package

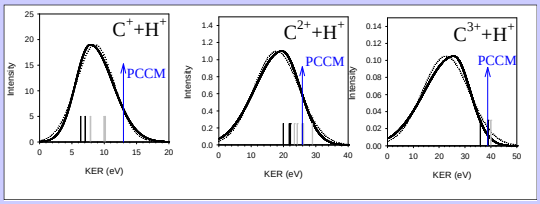

Comparison between measured and calculated KER-H^+

Dynamics associated to Auger relaxation

1s ionization contributes to 80% to the CH^{4+} production cross section
The dynamics of relaxation of the 1s hole, of the order of 10fs in $C^{(+/++)}$, strongly influences the KER value, as calculated within the PCCM model (figure below)

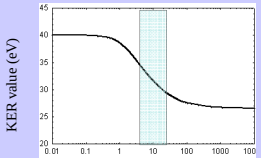

Lifetime of the 1s hole in CH^{+++} (fs)

Partitioning of energy in $(C_3H)^{++}$

Partitioning of energy in the fragmentation of $(C_3H)^{++}$ amongst 4 channels: C_3^+/H^+ (short dashed line), $C_2/C^+/H^+$ (dash-dot line), $C_2/C/H^+$ (solid line) and $C/C/C/H^+$ (dotted line).

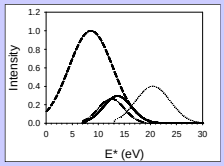

$E^*=E_{formation}$ + KER-H^+